The bigger picture: developing a graphical user interface to process UAV imagery of tidal stream environments

J. Slingsby, B. E. Scott, L. Kregting, J. McIlvenny, J. Wilson, M. Yanez and B. J. Williamson

Abstract—**Unmanned Aerial Vehicles (UAVs), or drones, offer the ability to collect cost-effective fine-scale imagery that is suitable for the capture of concurrent turbulence and faunal data within tidal stream environments. This is a necessary stage of information gathering to inform tidal energy device design, advise control and maintenance strategies and better inform environmental consenting processes.**

For this study a total of sixty-three UAV surveys were undertaken within the Inner Sound of the Pentland Firth, Scotland, UK, over two 4-day periods in 2016 and 2018. The aims of this data collection effort were to characterise bathymetrically driven turbulence features, including distribution, presence, and area, as well as marine life such as seabird distributions, presence, and orientation relative to the flow. To achieve this, a method to extract quantifiable metrics from UAV imagery was required.

This paper details the processes and methodology to create a graphical user interface (GUI) to provide these outputs rather than examining specific results. It includes an explanation of the criteria that the GUI needed to meet to be able to process the imagery, a description of the workflow and an explanation of the sub-routines required such as image registration and calibration. The outputs of the GUI, and their relevance to tidal energy developments, are also discussed. Finally, this paper details future work incorporating machine learning techniques to improve the accuracy, reliability, and processing speed of the GUI.

Keywords—**environmental monitoring, turbulence, seabirds, tidal turbines, image processing, drones**

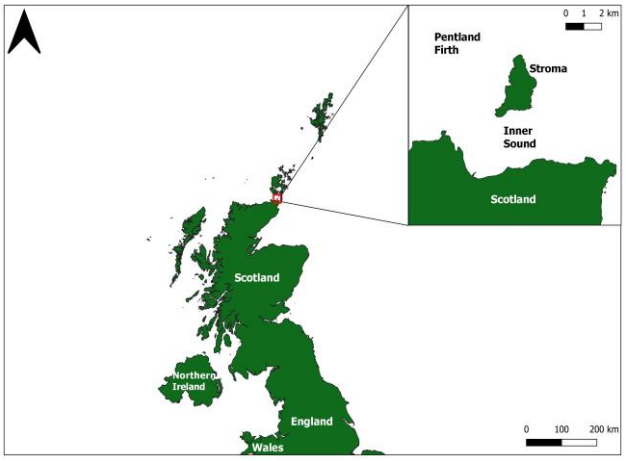

Fig. 1. The Inner Sound area of the Pentland Firth, Scotland, UK.

I. Introduction

UNMANNED aerial vehicles (UAVs), colloquially known as drones, are increasingly being utilised within the scientific community for a diverse range of research purposes [1]. Battery powered multirotor UAVs, characterised by being highly manoeuvrable and able to hover and vertically take-off, are a particularly attractive option for carrying out fine-scale (<1 m and <1 min) photogrammetric assessments across a range of distances from targets of interest [2].

Remotely sensed imagery is a permanent data set that can be referenced to or reanalysed in the future [3]. Image

Manuscript submitted 2 November, 2021; revised 15 November 2022; accepted 23 November 2022, published 31 March 2023.

This work was funded by the Bryden Centre project, supported by the European Union's INTERREG VA Programme, and managed by the Special EU Programmes Body (SEUPB). The views and opinions expressed in this paper do not necessarily reflect those of the European Commission or the Special EU Programmes Body (SEUPB). Aspects of this research were also funded by a Royal Society Research Grant [RSG\R1\180430] and the NERC VertIBase project [NE/N01765X/1].

J. Slingsby is with the Environmental Research Institute, University of the Highlands and Islands (UHI), Thurso KW14 7EE, UK (e-mail: james.slingsby@uhi.ac.uk).

B. E. Scott is with the School of Biological Sciences, University of Aberdeen, Aberdeen AB24 2TZ, UK (e-mail: b.e.scott@abdn.ac.uk)

L. Kregting is with the Queen's University Marine Laboratory, Queen's University Belfast, Portaferry BT22 1PF, UK (email: l.kregting@qub.ac.uk)

J. McIlvenny is with the Environmental Research Institute, University of the Highlands and Islands (UHI), Thurso KW14 7EE, UK (e-mail: jason.mcilvenny@uhi.ac.uk).

J. Wilson is with Marine Scotland Science, Marine Laboratory, Aberdeen AB11 9DB, UK (e-mail: jared.wilson.gov.scot).

M. Yanez was with the Institut National des Sciences Appliquées de Lyon, 69621 Lyon, France (e-mail: marionyanez@hotmail.fr)

B. J. Williamson is with the Environmental Research Institute, University of the Highlands and Islands (UHI), Thurso KW14 7EE, UK (e-mail: benjamin.williamson@uhi.ac.uk).

Digital Object Identifier: https://doi.org/10.36688/imej.6.11-17

processing tools allow for the extraction of relevant metrics and is a rapidly evolving field with computer vision enabling the development of increasingly autonomous techniques [4]. However, at the basis of any image processing tool a graphical user interface (GUI) is required. A GUI allows a user to manipulate, implement georectification, save/load and extract relevant features from imagery [5]. As a result, a GUI can allow for a highly customisable approach to the quantification of UAV derived data.

Tidal stream environments are areas where UAVs and image processing show great promise, with usage already highlighting success for environmental studies [6]–[11]. Tidal-stream environments are characterised as turbulent areas of marine coastline that produce predictable high current velocities greater than 1 m/s [12]. These environments are highly heterogeneous in nature, due to site-specific topography and bathymetry, and produce complex, ephemeral, turbulent features that vary across fine spatio-temporal scales (<10 m and <1 min) [13].

Characterisation of turbulence is of importance to tidal energy developers to inform turbine design, control and maintenance strategies, micro-siting and environmental consenting processes [14]. It is also key to understanding biophysical interactions occurring within the environment itself. This is because tidal stream environments have predictable, and localised, areas of prey which are then heavily utilised by foraging top predator species, such as seabirds and marine mammals [13].

UAV imagery therefore offers a cost-effective, and practical, way to capture turbulence and faunal data simultaneously at the surface [6], [15]. However, for data to be applicable, relevant embedded information must be extracted from what is essentially just a 'digital photograph'. To achieve this, a GUI was developed to process imagery taken from UAV surveys within the Inner Sound area of the Pentland Firth, Scotland, UK. This allowed for the final output to be achieved: extraction of georeferenced, quantifiable metrics of turbulence and faunal targets, hereafter known as objects of interest (OOI), which could be analysed relative to pertinent environmental covariates.

The aim of this paper is to detail the steps and individual processes involved (from input to output), the implications of the results to relevant stakeholders and future work to enhance development.

II. Methods

A. Study Site

Due to proximity with the Environmental Research Institute (approx. 15 km), and being host to the MeyGen tidal energy project, the Inner Sound, within the Pentland Firth, was chosen as the study site for this work (Fig. 1.). The Pentland Firth is a large channel (c. 20 km wide) of water that separates mainland Scotland and the Orkney Isles in the UK and connects the North Atlantic and the North Sea [16]. The Inner Sound is a contributing channel of this, with an average depth of approximately 30 m [17]. Due to a large variance in tidal phase when moving from either entrance of the channel, and topographic features, recorded current velocities can exceed 3 m/s [18]. During flood spring tides, current speeds have been recorded to reach 6 m/s, with an estimated energy potential of around 1.9 GW [17].

These conditions make the Inner Sound one of the most prominent tidal lease sites both within the UK and globally. Currently it includes the MeyGen project owned by SIMEC Atlantis Energy. This has a total planned capacity of 398 MW and since 2017 has installed four 1.5 MW turbines outputting over 43 GWh in total energy generation as of July 2022 [19].

B. Data Collection

In total sixty-three UAV surveys were conducted within the Inner Sound over four-day periods, across differing phases of the tidal cycle (ebb/flood), in both 2016 (23-25th June) and 2018 (21-24th July). For both years standard flight durations were 10-30 min with approx. 200 images taken each time. While this was achieved using different UAV, camera type, flight height, image type and sampling interval between the two years (Table. I.), these did not impact the overall aim of quantifying OOIs from within the imagery as will be discussed in section II E. All flights were undertaken in line with the current regulations, set out by the Civil Aviation Authority (CAA) for drone operation, as well as using current recommended best practise guidelines for UAV usage within scientific research [20], [21].

UAV take-off occurred from a consistent location on the deck of the MRV Scotia, of a known height above sea level (10.6 m). During operation, all surveys were manually flown at a consistent positioning (100 m) and speed ahead of the vessel. This allowed for vessel-based observers to maintain visual contact with the UAV to note when OOIs were under the drone. It was also done to comply with CAA regulations of flying within visual line of sight (<500 m). For safety, flights only occurred at windspeeds <5 m/s, which was significantly lower than the recommended value suggested by the UAV manufacturer [22]. All flights were conducted against the prevailing current direction to avoid the miscounting of OOIs and to better account for the movement of water under the drone's field of view (FOV). All flights were conducted during daylight hours.

TABLE I
COMPARISON OF UAV CAMERA SPECIFICATIONS AND SAMPLING METHODS BETWEEN 2016 AND 2018 SURVEYS.

UAV and Camera Specifications	2016	2018
UAV	SwellPro SplashDrone 3+	DJI Phantom 4 Advanced V2.0
Camera	GoPro HERO4 Black (12 MP)	1-inch CMOS Sensor (20 MP)
Aspect Ratio	4:3 (4000 x 3000 pixels)	3:2 (5472 x 3648 pixels)
Average relative altitude flown	46 m	70 m
Image type taken	JPEG	Simultaneous pairs of RAW and JPEG
Sampling interval between images/ image pairs	1 second (subsampled to match 2018 data)	5 seconds

C. *Image Registration*

To align the UAV images in space, each image needed to undergo a process called image registration. On-board telemetry data was used to obtain altitude, heading, and coordinate (of the central point) values of each individual image, for each flight undertaken. Pitch and roll values were not needed due to the stabilisation from the gimbal-mounted camera. These values were extracted from image's extensible metadata platform (XMP) data (embedded metadata contained within each image). Relative altitude (relative to the take-off altitude) was corrected to absolute altitude to obtain the actual elevation above mean sea level using the take-off height. The observation deck, utilised as the launch point, was a standard and known height (10.6 m above sea level), and used for this purpose. Once registration was completed a second sub-routine was developed to convert the pixel length in an image into metres.

D. *Calibration Factor*

To negate the difference in UAV model, flight height, and camera type between the two years, and to maximise the accuracy of OOI measurements, a calibration factor was required. The purpose of this was to convert the standard scale of images (pixels) into a useable distance metric (metres). A unique calibration factor was required per image, as opposed to for each survey, as UAV altitude varied slightly in each image around the mean flight height recorded. Equations (1), (2) and (3) were used to achieve this. These calculations, implemented in MATLAB 2019b, converted pixels into metres utilising the length and width of the image in pixels, the relative altitude of the UAV (when that image was taken) and the vertical field of view (VFOV) of the camera.

$$tan\,(VFOV\backslash 2) = Width[m]/(2 \times Altitude) \quad (1)$$

$$Width[m] = (2 \times Altitude) \times tan(VFOV/2) \quad (2)$$

$$Calibration\ factor = Width[m]/Width[px] = (2 \times Altitude) \times tan(VFOV/2)/Width[px] \quad (3)$$

E. *Image Coverage*

To be able to view the physical area over ground, UAV coverage from hereon, the corner coordinates of each individual image had to be determined. However, the image registration process only provided the centre point of each image. Factors that had to be considered included spatial overlap (the distance between each image), image orientation and the footprint of each picture. Using the function "reckon()", within MATLAB 2019b, it was possible to compare the image centre point against that of another, and calculate the distance, in metres, between them. The function finds the coordinates of a point at a specified distance and azimuth from a starting point with coordinates. This function was also able to utilise heading values, from XMP data, to allow for an image's orientation, in space, to be properly displayed. By using the camera specifications, in this case pixel length/width and vertical field of view (VFOV), in combination with overlap and heading values, it was possible to represent each image as a polygon. To do this the distance in metres between the centre and the corners of each image had to be calculated. This was equal to the distance in pixels multiplied by the image calibration factor that considered the earth's radius (to account for the curvature of the earth), UAV relative altitude/heading and the size in pixels of the image in question.

With this information, the MATLAB 2019b function "kmlwritepolygon()" was then implemented to create a geographical polygon for each image in the form of a Keyhole Markup Language (KML) file. This function writes the geographic latitude and longitude data that define the polygon vertices, to a specified file in the KML format. As a result, an Excel spreadsheet containing image name and coordinates of the corner positions was recorded. Finally, using the software QGIS, these Excel files were combined and converted into a shapefile to provide a graphical output of the total survey coverage (Fig. 2.). This was carried out for all surveys that were processed within the GUI.

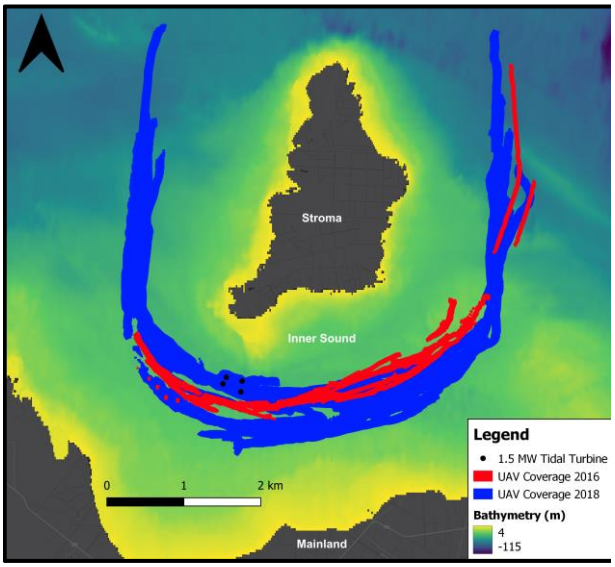

Fig. 2. UAV area coverage of all surveys carried out in both 2016 and 2018.

III. GUI Workflow

A. Objectives

To extract quantifiable information about turbulence features and marine fauna from UAV-derived imagery, several criteria had to be met. Firstly, multiple images, within a single survey, had to be collated to allow for the tracking of OOI between images to avoid misidentification and overestimation. Secondly, it needed to be possible to annotate images with information including: OOI location, number, classification and then take relevant measurements from the target. Finally, this had to be stored in an Excel file output, alongside relevant image/telemetry information, for succinct data analysis and presentation.

B. Initialisation

Before accessing the GUI an initialisation process, developed in MATLAB 2019b, was completed. This implemented necessary sub-routines (image registration, image coverage and calibration factor) and displayed key GUI variables (Fig. 3.). If any sub-routines were missing the user was asked to enter the correct file path for these functions before moving forward.

If all related functions were found, the initialisation process asked the user to select the image folder to process. After the image folder was selected the registration sub-routine ran and the framework of the output table was created. This contained each image name, a time stamp and the relevant telemetry data previously described in the image registration section. At this point the user was asked to input the height of the launch point for relative altitude to be calculated. Finally, the initialisation process asked the user to select a location to name and save the overall output file. If the file name already existed in this location a dialog box asked the user if they wished to restart or continue from the last image viewed within that folder. The GUI was activated once the initialisation process ended, culminating in the last stage of the entire workflow (Fig. 3.).

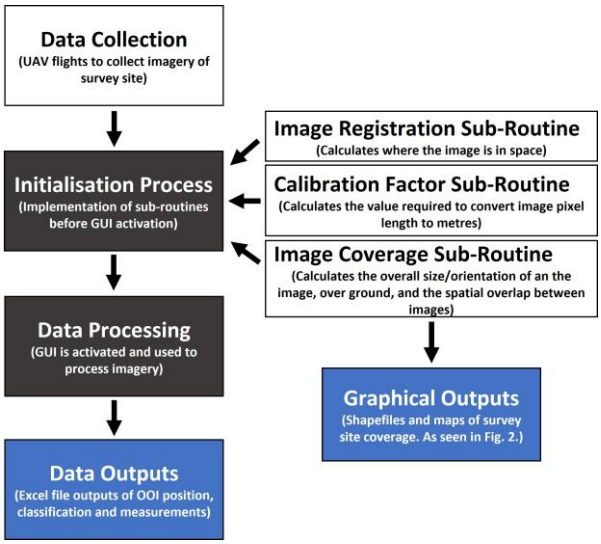

Fig. 3. The complete workflow of imagery collection and GUI usage, detailing the inputs (white), processes (black) and outputs (blue).

C. Data Processing

The GUI itself (Fig. 4.), developed within MATLAB 2019b, using code developed from the GUI Layout Toolbox, allowed a user to sequentially move through all images within a selected folder and log an unlimited number of OOIs [23]. The user could click and mark the estimated central point of each OOI thus obtaining a positional measurement (in pixel coordinates) (Fig. 4.). Drawing functions then facilitated the measurement of length and area (in pixels) (Fig. 4.). A menu then allowed for that OOI's characteristics to be registered. The information that was recorded here included a classification (faunal species or turbulence type), a confidence factor related to how certain the user was with

that identification, and if the OOI was present on the previous image (Fig. 4.). Once stored, this information could be saved temporarily, within the GUI memory itself, to allow for editing, before being inputted into the final Excel output file. If any classification or measurement information was missing, the GUI was able to alert the user to this. Finally, the GUI allowed for the flexibility to delete the previous click, and measurements, and to permanently delete information about a specific OOI from the GUI memory entirely.

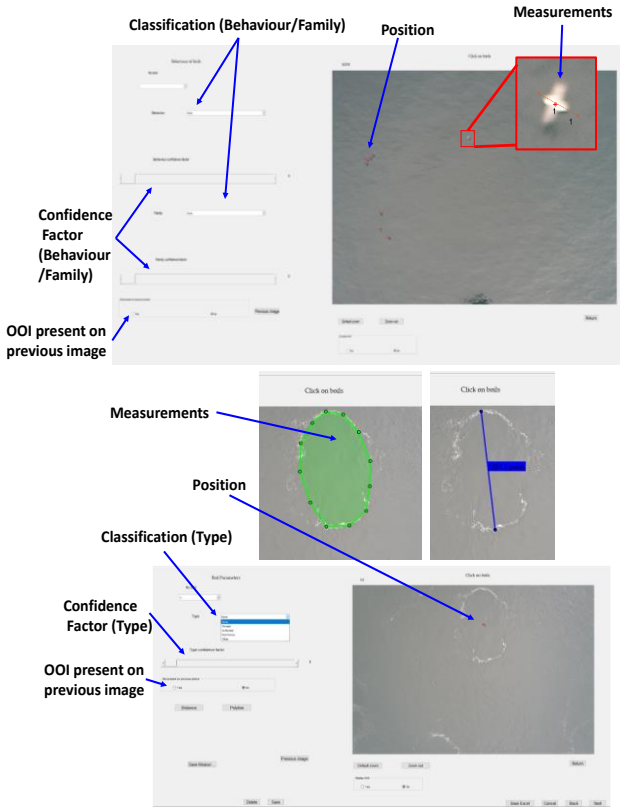

Fig. 4. Examples of the GUI display presented to users when processing imagery, highlighting the ability to record both faunal (top image) and turbulence (bottom image) data.

IV. Discussion

The use of UAVs to capture fine-scale imagery of tidal stream environments, and relevant OOI, is an emerging and highly novel, area of research. It can provide a new perspective, comparative to existing ecological and physical survey methods, as it has the capability of capturing fine-scale turbulence and faunal data concurrently. Data collection requires a specific method to extract quantifiable metrics. The developed GUI (Fig. 4.) allows for a tailored approach to the extraction, and quantification, of UAV imagery from within a tidal stream environment to be achieved. The type of output includes OOI position, classification, and relevant measurements. These can be visually displayed or included in analysis against relevant environmental variables. This offers a user-friendly tool, for relevant stakeholders, to process and analyse photogrammetric assessments of tidal stream environments in a relatively short timeframe (hours/days). As shown in this paper, the GUI is also not site or equipment limited, with simple alterations to camera specifications within the code allowing compatibility with most downward facing cameras in any environment.

The outputs created by the GUI have implications for tidal energy developers and regulators. The technique was demonstrated in a recent paper, which characterised turbulent feature (kolk-boil) distribution, presence, and area at the surface, and discussed relevance for tidal stream turbines and foraging seabirds [11]. Kolk-boils are formed through the interaction of water flow and bathymetry, creating vortices that move upward through the water column which erupt at the surface as smooth patches of water encompassed by a visible perimeter [24]. Characterisation of kolk-boils is key to micro-siting and for the development of turbines themselves as sustained turbulence will have a detrimental effect on the longevity and reliability of material components, compared to laminar flow conditions [14]. The collection of fine-scale (metres and seconds), empirical, turbulence data is therefore a crucial aspect of habitat characterisation assessments for tidal energy devices. The outputs of the GUI can facilitate this, providing enough information to create individual datasets that stand alone or which can be complementary to a larger collection effort. To allow for wider public useability, code will be transitioned to R and Python.

We also highlight that the GUI provides the ability to gain accurate positional data, and other fine-scale measurements (metres and seconds), of animals at the surface. These outputs can provide further understanding into fine-scale animal usage patterns and interactions with previously described turbulent features [7]. This is important for understanding the bio-physical interactions occurring within the habitat, and to be able to fully describe the potential effects of tidal energy developments throughout deployment and operational lifecycle for required environmental assessments [15].

While the GUI was able to produce highly relevant outputs from UAV imagery, there are areas that can still be enhanced and developed. The main drawback to manual image processing, is the time (hours and days) required to systematically process through large UAV imagery datasets manually. Although this allows for the creation of quantifiable metrics, not achievable through simple observation of the images, this can be a significant bottleneck that can negate using a UAV to increase surveying efficiency in the first place [25]. However, machine learning techniques are a rapidly developing area that offer an ability to address this [4].

Machine learning involves the incorporation of algorithms that are trained to automatically detect and classify OOIs [26]. Deep learning is a form of machine

learning that utilises artificial neural networks to learn directly from the data, meaning it can automatically extract relevant features unlike conventional methods where this must be done manually as part of a training process [27]. These methods are also capable of "end-to end learning" where an algorithm will autonomously learn how to achieve a given task and will develop its own way to achieve this [28]. A recent study using UAV imagery found that when using deep learning techniques, to detect seabirds on the water, accuracy of overall classification (of true positives) reached 98% [29]. Finally, deep learning algorithms, can learn from previous inputs and are able to refine techniques with the more information that it is given [28].

Machine and deep learning algorithms could be used to decrease the time taken to locate images containing OOI within datasets. Automated filtering would decrease data processing times (days/hours to minutes) by detecting images containing OOIs and only allowing those to be put forward for further analysis. This would allow for an effective addition of automation that would complement the existing GUI infrastructure.

V. Conclusion

In conclusion, a user-friendly graphical user interface was developed to allow for a tailored approach to processing fine-scale UAV imagery of a tidal stream environment. This permitted the processing of imagery containing concurrent turbulent features (kolk-boils), and faunal targets (seabirds and marine mammals), and has led to the ability to gain quantifiable metrics with regards to position, classification, and measurements at the surface. These can then be examined in relation to pertinent environmental variables and utilised to further explore biophysical interactions occurring within these environments and to aid in the continued development of tidal energy devices through habitat characterisation. This has already been observed with the methodology producing published insights into the characterisation of turbulent features at the surface and interactions of diving seabirds with them.

However, this GUI is not solely restricted to tidal stream environments and can be easily manipulated for use with alternative downward facing camera specifications. With the aid of deep learning techniques this tool will also continue to be developed in its efficiency, and accuracy, of processing large UAV imagery data sets.

Acknowledgement

We gratefully acknowledge the support of Julien Martin, colleagues at Marine Scotland Science, the crew and scientists of the MRV Scotia 2016 and 2018 cruises (particularly Chief Scientists Eric Armstrong and Adrian Tait), and ERI interns: Gael Gelis and Martin Forestier. We thank the reviewers for the constructive comments that have aided in the improvement of this paper.

References

[1] C. Stöcker, R. Bennett, F. Nex, M. Gerke, and J. Zevenbergen, 'Review of the Current State of UAV Regulations', *Remote Sens (Basel)*, vol. 9, no. 5, p. 459, May 2017, doi: 10.3390/rs9050459.

[2] A. P. Colefax, P. A. Butcher, and B. P. Kelaher, 'The potential for unmanned aerial vehicles (UAVs) to conduct marine fauna surveys in place of manned aircraft', *ICES Journal of Marine Science*, vol. 75, no. 1, pp. 1–8, 2018, doi: 10.1093/icesjms/fsx100.

[3] D. Chabot and C. M. Francis, 'Computer-automated bird detection and counts in high-resolution aerial images: a review', *Journal of Field Ornithology*, vol. 87, no. 4. Wiley/Blackwell (10.1111), pp. 343–359, Dec. 01, 2016. doi: 10.1111/jofo.12171.

[4] T. Hollings, M. Burgman, M. van Andel, M. Gilbert, T. Robinson, and A. Robinson, 'How do you find the green sheep? A critical review of the use of remotely sensed imagery to detect and count animals', *Methods Ecol Evol*, vol. 9, no. 4, pp. 881–892, Apr. 2018, doi: 10.1111/2041-210X.12973.

[5] Q. Deng and X. Chen, 'An image processing toolbox based on MATLAB GUI', in *Journal of Physics: Conference Series*, Sep. 2021, vol. 2010, no. 1. doi: 10.1088/1742-6596/2010/1/012137.

[6] L. Lieber, W. A. M. Nimmo-Smith, J. J. Waggitt, and L. Kregting, 'Localised anthropogenic wake generates a predictable foraging hotspot for top predators', *Commun Biol*, vol. 2, no. 1, p. 123, 2019, doi: 10.1038/s42003-019-0364-z.

[7] J. Slingsby *et al.*, 'Using unmanned aerial vehicle (UAV) imagery to characterise pursuit- diving seabird association with tidal stream hydrodynamic habitat features', *Front Mar Sci*, vol. 9, no. March, pp. 1–17, 2022, doi: 10.3389/fmars.2022.820722.

[8] L. Lieber, R. Langrock, and A. Nimmo-Smith, 'A bird's eye view on turbulence: Seabird foraging associations with evolving surface flow features', *Proceedings of the Royal Society B*, vol. 288, no. 1949, p. rspb.2021.0592, Apr. 2021, doi: 10.1098/rspb.2021.0592.

[9] J. McIlvenny *et al.*, 'Comparison of dense optical flow and PIV techniques for mapping surface current flow in tidal stream energy sites', *International Journal of Energy and Environmental Engineering*, pp. 1–13, Sep. 2022, doi: 10.1007/S40095-022-00519-Z/FIGURES/8.

[10] I. Fairley *et al.*, 'Drone-based large-scale particle image velocimetry applied to tidal stream energy resource assessment', *Renew Energy*, vol. 196, pp. 839–855, Aug. 2022, doi: 10.1016/J.RENENE.2022.07.030.

[11] J. Slingsby *et al.*, 'Surface Characterisation of Kolk-Boils within Tidal Stream Environments Using UAV Imagery', *J Mar Sci Eng*, vol. 9, no. 5, p. 484, Apr. 2021, doi: 10.3390/jmse9050484.

[12] L. Lieber, W. A. M. Nimmo-Smith, J. J. Waggitt, and L. Kregting, 'Fine-scale hydrodynamic metrics underlying predator occupancy patterns in tidal stream environments', *Ecol Indic*, vol. 94, pp. 397–408, Nov. 2018, doi: 10.1016/j.ecolind.2018.06.071.

[13] S. Benjamins *et al.*, 'Confusion reigns? A review of marine megafauna interactions with tidal-stream environments', *Oceanography and Marine Biology: An Annual Review*, vol. 53, pp. 1–54, 2015, doi: 10.1201/b18733-2.

[14] M. Thiébaut *et al.*, 'A comprehensive assessment of turbulence at a tidal-stream energy site influenced by wind-generated ocean waves', *Energy*, vol. 191, p. 116550, Jan. 2020, doi: 10.1016/j.energy.2019.116550.

[15] N. Isaksson *et al.*, 'Assessing the effects of tidal stream marine renewable energy on seabirds: A conceptual

framework', *Mar Pollut Bull*, vol. 157, no. March, 2020, doi: 10.1016/j.marpolbul.2020.111314.

[16] L. Goddijn-Murphy, D. K. Woolf, and M. C. Easton, 'Current patterns in the inner sound (Pentland Firth) from underway ADCP data', *J Atmos Ocean Technol*, vol. 30, no. 1, pp. 96–111, Jan. 2013, doi: 10.1175/JTECH-D-11-00223.1.

[17] M. C. Easton, D. K. Woolf, and P. A. Bowyer, 'The dynamics of an energetic tidal channel, the Pentland Firth, Scotland', *Cont Shelf Res*, vol. 48, pp. 50–60, Oct. 2012, doi: 10.1016/j.csr.2012.08.009.

[18] J. McIlvenny, D. Tamsett, P. Gillibrand, and L. Goddijn-Murphy, 'On the sediment dynamics in a tidally energetic channel: The Inner Sound, Northern Scotland', *J Mar Sci Eng*, vol. 4, no. 2, p. 31, Apr. 2016, doi: 10.3390/jmse4020031.

[19] Tethys, 'MeyGen Tidal Energy Project - Phase I | Tethys', 2022. https://tethys.pnnl.gov/project-sites/meygen-tidal-energy-project-phase-i (accessed Oct. 27, 2022).

[20] J. C. Hodgson *et al.*, 'Drones count wildlife more accurately and precisely than humans', *Methods Ecol Evol*, 2018, doi: 10.1111/2041-210X.12974.

[21] Civil Aviation Authority, 'UK CAA Drone Code', 2019. https://dronesafe.uk/wp-content/uploads/2019/11/Drone-Code_October2019.pdf

[22] DJI, 'DJI Phantom 4 Pro – Specs, Tutorials & Guides – DJI', 2020. https://www.dji.com/uk/phantom-4-pro/info#specs (accessed Jul. 17, 2020).

[23] D. Sampson, 'GUI Layout Toolbox', *MATLAB Central File Exchange*, 2022. https://uk.mathworks.com/matlabcentral/fileexchange/47982-gui-layout-toolbox (accessed Nov. 02, 2022).

[24] J. Dufaur, 'Characteristics of the turbulent flow in the Inner Sound, tidal development site in the Pentland Firth, Scotland.', Master's Thesis, University of Aberdeen, 2016.

[25] U. K. Verfuss *et al.*, 'A review of unmanned vehicles for the detection and monitoring of marine fauna', *Marine Pollution Bulletin*, vol. 140. pp. 17–29, Mar. 2019. doi: 10.1016/j.marpolbul.2019.01.009.

[26] C. Martin, S. Parkes, Q. Zhang, X. Zhang, M. F. McCabe, and C. M. Duarte, 'Use of unmanned aerial vehicles for efficient beach litter monitoring', *Mar Pollut Bull*, vol. 131, pp. 662–673, Jun. 2018, doi: 10.1016/J.MARPOLBUL.2018.04.045.

[27] S. Skansi, *Introduction to Deep Learning*. Springer Nature, 2018. doi: 10.1007/978-981-13-6794-6_1.

[28] MathWorks, 'What Is Deep Learning? | How It Works, Techniques & Applications - MATLAB & Simulink', 2019. https://www.mathworks.com/discovery/deep-learning.html (accessed Jan. 28, 2021).

[29] L. Ben Boudaoud, F. Maussang, R. Garello, and A. Chevallier, 'Marine Bird Detection Based on Deep Learning using High-Resolution Aerial Images', in *OCEANS 2019-Marseille*, 2019, no. June, pp. 1–7. doi: 10.1109/oceanse.2019.8867242.